



# Audio Engineering Society Convention Paper

Presented at the 138th Convention  
2015 May 7–10 Warsaw, Poland

*This paper was peer-reviewed as a complete manuscript for presentation at this Convention. Additional papers may be obtained by sending request and remittance to Audio Engineering Society, 60 East 42<sup>nd</sup> Street, New York, New York 10165-2520, USA; also see [www.aes.org](http://www.aes.org). All rights reserved. Reproduction of this paper, or any portion thereof, is not permitted without direct permission from the Journal of the Audio Engineering Society.*

## Discussion of the Wavefront Sculpture Technology Criteria for Straight Line Arrays

Frank Schultz<sup>1</sup>, Florian Straube<sup>2</sup>, and Sascha Spors<sup>1</sup>

<sup>1</sup>*Institute of Communications Engineering, University of Rostock, Germany*

<sup>2</sup>*Audio Communication Group, TU Berlin, Germany*

Correspondence should be addressed to Frank Schultz ([frank.schultz@uni-rostock.de](mailto:frank.schultz@uni-rostock.de))

### ABSTRACT

Wavefront Sculpture Technology introduced line source arrays for large scale sound reinforcement, aiming at the synthesis of highly spatial-aliasing free sound fields for full audio bandwidth. The paper revisits this technology and its criteria for straight arrays using a signal processing model from sound field synthesis. Since the latest array designs exhibit very small driver distances, the sampling condition for grating lobe free electronic beam forming regains special interest. Furthermore, a discussion that extends the initial derivations of the spatial lowpass characteristics of circular and line pistons, and line pistons with wavefront curvature applied in subarrays is given.

### 1. INTRODUCTION

In [1, 2] we started to revisit the Wavefront Sculpture Technology<sup>1</sup> (WST) [3, 4, 5] that constitutes the fundamentals of line array technology for full audio bandwidth public address. An acoustic signal processing model initially developed for sound field synthesis (SFS) [6, 7, 8, 9] was utilized, that is also well known in array processing and antenna theory [10, 11]. In essence, the first three WST criteria deal

with the avoidance or attenuation of grating lobes in the farfield radiation pattern of straight line source arrays (LSA), which consequently avoids or reduces spatial aliasing in the Fresnel and Fraunhofer region. In this paper we revisit these WST criteria and give some extended analysis. The WST criteria under discussion are summarized as, cf. [5, p.929]:

The *active radiating factor* (ARF) criterion

$$\text{WST \#1:} \quad \text{ARF} = \frac{l}{\Delta y} \geq 0.82 \quad (1)$$

for a uniformly driven, straight LSA relates the discretization step  $\Delta y$  between adjacent line pistons

<sup>1</sup>Wavefront Sculpture Technology<sup>®</sup> is a registered trademark of L-ACOUSTICS US, LLC. We omit the labeling in the remainder of the paper and will only use the relevant research results.

with individual length  $l$  and a tolerated grating lobe level (i.e. the occurrence of spatial aliasing). The criterion ensures, that the maximum grating lobe level does not exceed -13.5 dB relative to the intended main lobe and holds for a large number of active line pistons. The criterion aims at avoiding or reducing spatial aliasing by utilizing the spatial lowpass characteristics of highly directive sources, i.e. waveguides.

The 2<sup>nd</sup> WST criterion

$$\text{WST \#2:} \quad \Delta y < \frac{\lambda_{\min}}{2} \quad (2)$$

is the general spatial baseband sampling condition. It ensures complete grating lobe avoidance for electronically steered arrays built from spherical monopoles with the highest operating frequency  $f_{\max} = c/\lambda_{\min}$  denoting the speed of sound  $c = 343$  m/s and the wave length  $\lambda$  in m. In [5, p.917] the criterion was derived in order to avoid strong off-axis lobes for a uniformly driven LSA. The criterion limits the temporal frequency bandwidth – matching the spatial base band – of the loudspeaker's driving function in order to avoid spatial aliasing.

The 3<sup>rd</sup> WST criterion relates an occurring wavefront curvature of horns, i.e. the arc in Fig. 1 and a tolerated grating lobe level for an LSA built without gaps between the horns. For the so called sagitta  $S$

$$\text{WST \#3:} \quad S < \frac{\lambda_{\min}}{4}, \quad (3)$$

must hold in order that the LSA exhibits a grating lobe attenuation larger than 10 dB relative to the intended main lobe, cf. [5, Fig. 9,10], [12, Fig. 19]. This criterion also aims at reducing spatial aliasing by utilizing the spatial lowpass characteristics of the sources that construct the LSA.

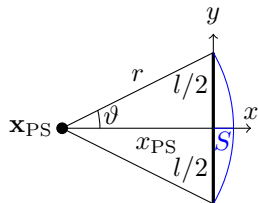


Fig. 1: Geometry for the wavefront curvature model, cf. [5, Fig. 8], [13, Fig. 38].

## 2. WST SIGNAL PROCESSING MODEL

For convenience the WST signal processing model is shortly revisited here, the nomenclature and conventions of [2] are used. The model is depicted in Fig. 2, given in the temporal and spatio-temporal Fourier spectrum domain. The spatio-temporal spectrum  $P(k_y, \omega)$  of a sound pressure function over space and time  $p(y, t)$  is given by the Fourier transform

$$P(k_y, \omega) = \int_{-\infty}^{+\infty} \int_{-\infty}^{+\infty} p(y, t) e^{+j k_y y} dy e^{-j \omega t} dt, \quad (4)$$

its inverse reads

$$p(y, t) = \frac{1}{4 \pi^2} \int_{-\infty}^{+\infty} \int_{-\infty}^{+\infty} P(k_y, \omega) e^{-j k_y y} dk_y e^{+j \omega t} d\omega. \quad (5)$$

In the remainder only temporal, e.g.  $P(x, y, \omega)$  and spatio-temporal spectra, e.g.  $P(x, k_y, \omega)$  are considered. A monochromatic propagating sound field with angular temporal frequency  $\omega_0$  and corresponding wave length  $\lambda_0 = \frac{2 \pi c}{\omega_0}$  is assumed. Thus, the term  $2 \pi \delta(\omega - \omega_0)$  is omitted in all temporal and spatio-temporal spectra.

The LSA is located on the  $y$ -axis with  $y_0$  indicating a position within the array. The  $xy$ -plane for  $x > 0$  is considered as the the sound field synthesis region, thereby ignoring the horizontal radiation characteristics of the LSA, cf. [14, Sec. 4].

Following the signal processing model, the spatio-temporal spectrum of the sound pressure  $P(x, k_y, \omega)$  can be obtained by different driving functions' spatio-temporal spectra

$$P(x, k_y, \omega) = \left\{ \begin{array}{l} D(k_y, \omega) \\ D_w(k_y, \omega) \\ D_{w,S}(k_y, \omega) \\ D_{w,S,H}(k_y, \omega) \end{array} \right\} \cdot G_0(x, k_y, \omega). \quad (6)$$

$D(k_y, \omega)$  models an infinite, continuous LSA;  $D_w(k_y, \omega)$  a finite length, continuous LSA;  $D_{w,S}(k_y, \omega)$  a finite length, discretized LSA built from spherical monopoles and  $D_{w,S,H}(k_y, \omega)$  a finite length, discretized LSA built from identical baffled pistons.

$G_0(x, k_y, \omega)$  is the spatio-temporal spectrum of the 3D free-field Green's function

$$G(\mathbf{x}, \mathbf{x}_0, \omega) = \frac{1}{4 \pi} \frac{e^{-j \frac{\omega}{c} \|\mathbf{x} - \mathbf{x}_0\|}}{\|\mathbf{x} - \mathbf{x}_0\|} \quad (7)$$

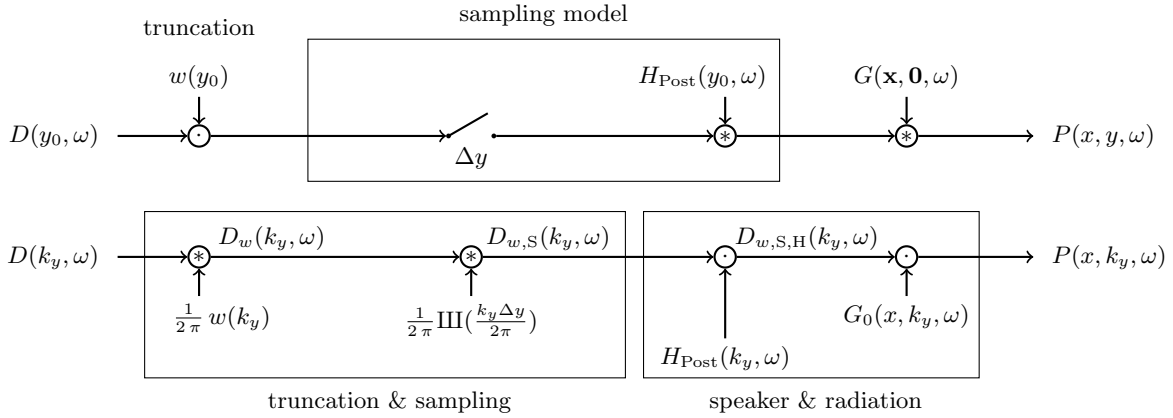


Fig. 2: WST signal processing model. Representation in temporal (top) and spatio-temporal spectrum domain (bottom). Convolution w.r.t.  $y$  is denoted by  $\circledast$  (not to be confused with the circular convolution), multiplication w.r.t.  $k_y$  by  $\odot$ .

of the Helmholtz equation, placed at the origin  $\mathbf{x}_0 = \mathbf{0}$  [15, (52)].

The initial derivations of the WST criteria consider a uniformly driven and rectangular truncated LSA. Thus, with unity gain normalization, the driving function for an infinite, continuous LSA reads

$$D(y_0) = 1 \circledast D(k_y, \omega) = 2\pi \delta(k_y), \quad (8)$$

indicating the spatial Fourier transform with the  $\circledast$  symbol. Spatial truncation with the rectangular window

$$w(y_0) = \begin{cases} \frac{1}{L} & \text{for } |y_0| \leq \frac{L}{2} \circledast \\ 0 & \text{else} \end{cases}$$

$$w(k_y) = \begin{cases} \frac{\sin(k_y \frac{L}{2})}{k_y \frac{L}{2}} & \text{for } k_y \neq 0 \\ 1 & \text{for } k_y = 0, \end{cases} \quad (9)$$

leads to the driving function of a finite length, continuous LSA

$$D_w(y_0) = \begin{cases} \frac{1}{L} & \text{for } |y_0| \leq \frac{L}{2} \circledast \\ 0 & \text{else} \end{cases}$$

$$D_w(k_y, \omega) = \begin{cases} \frac{\sin(k_y \frac{L}{2})}{k_y \frac{L}{2}} & \text{for } k_y \neq 0 \\ 1 & \text{for } k_y = 0. \end{cases} \quad (10)$$

Equidistant spatial sampling of the driving function

w.r.t. the discretization step  $\Delta y$  with  $\nu, \mu \in \mathbb{Z}$

$$\underbrace{\sum_{\nu=-\infty}^{+\infty} \delta(y_0 - \nu \Delta y)}_{=:\frac{1}{\Delta y} \text{III}(\frac{y_0}{\Delta y})} \circledast \underbrace{\frac{2\pi}{\Delta y} \sum_{\mu=-\infty}^{+\infty} \delta(k_y - \mu \frac{2\pi}{\Delta y})}_{=:\text{III}(\frac{k_y \Delta y}{2\pi})} \quad (11)$$

and spatial truncation leads to the driving function of the finite length, discretized array built from an odd number  $N$  of spherical monopoles

$$D_{w,S}(y_0) = \sum_{\nu=-\frac{N-1}{2}}^{+\frac{N-1}{2}} \frac{1}{N} \cdot \delta(y_0 - \nu \Delta y) \circledast$$

$$D_{w,S}(k_y, \omega) = \begin{cases} \frac{\sin(k_y \Delta y \frac{N}{2})}{N \sin(k_y \Delta y \frac{1}{2})} & \text{for } k_y \neq \frac{2\pi}{\Delta y} \mu \\ 1 & \text{for } k_y = \frac{2\pi}{\Delta y} \mu. \end{cases} \quad (12)$$

$D_{w,S}(k_y, \omega)$  is the so called aliased sinc function. For odd  $N$  it is periodic with the spatial sampling frequency  $k_{y,S} = \frac{2\pi}{\Delta y}$  and exhibits spectral repetitions of the 'base band'  $|k_y| \leq \frac{\pi}{\Delta y}$ . For  $\mu = 0$  the main lobe is obtained, for all other  $\mu$  grating lobes of the same level as the main lobe occur. This LSA configuration exhibits an equivalent length  $L = \Delta y N$ , that a continuous, finite length LSA would have.

The sampling model requires a spatial reconstruction filter to suppress the spectral repetitions. This

filter has to be applied in the acoustic domain. As spatial reconstruction filter  $H_{\text{Post}}(k_y, \omega)$ , the line piston on  $y$ -axis with length  $l$

$$H_{\text{Rect}}(y_0) = \begin{cases} \frac{1}{l} & \text{for } |y_0| \leq \frac{l}{2} \\ 0 & \text{else} \end{cases} \quad \circ \bullet$$

$$H_{\text{Rect}}(k_y, \omega) = \begin{cases} \frac{\sin(k_y \frac{l}{2})}{k_y \frac{l}{2}} & \text{for } k_y \neq 0 \\ 1 & \text{for } k_y = 0 \end{cases} \quad (13)$$

and the circular piston within the  $yz$ -plane with radius  $r_0$

$$H_{\text{Circ}}(y_0, z_0) = \begin{cases} \frac{1}{\pi r_0^2} & \text{for } y_0^2 + z_0^2 \leq r_0^2 \\ 0 & \text{else} \end{cases} \quad \circ \bullet$$

$$H_{\text{Circ}}(k_y, \omega) = \begin{cases} \frac{2 J_1(k_y r_0)}{k_y r_0} & \text{for } k_y \neq 0 \\ 1 & \text{for } k_y = 0 \end{cases} \quad (14)$$

were considered for the derivation of the first WST criterion, denoting the cylindrical Bessel function of 1<sup>st</sup> kind of 1<sup>st</sup> order [16, §10.2] with  $J_1(\cdot)$ . Under the assumption that the LSA is built from identical pistons, the driving function's spatio-temporal spectrum

$$D_{w,S,H}(k_y, \omega) = D_{w,S}(k_y, \omega) \cdot H_{\text{Post}}(k_y, \omega) \quad (15)$$

follows as a consequence of the product or pattern multiplication theorem [17, p.174], [10, Ch. 2.8].

Note that all driving function and postfilter Fourier transform pairs are chosen for amplitude normalization at  $k_y = 0$ , such that the main lobes exhibit unity gain. In doing so, relative grating and side lobe amplitudes can be conveniently discussed in terms of their absolute values.

The propagating part of  $G_0(x, k_y, \omega)$  is bounded and thus bandlimited to the region where  $|k_y| < \frac{\omega_0}{c}$  allows propagating wave synthesis. This is referred to as the *visible region* [10, Ch. 2.3] or *physical region* [3] of the array. Evanescent wave radiation occurs for  $|k_y| > \frac{\omega_0}{c}$ , this part of the spectrum is not bandlimited, however it is decaying rapidly for increased  $x$ . By restricting the spatio-temporal spectra of the driving functions to the visible region  $-\frac{\omega_0}{c} < k_y < +\frac{\omega_0}{c}$ , the nonlinear mapping between  $k_y$  and the propagating wave radiation angle  $\phi$

$$k_y = \frac{\omega_0}{c} \sin \phi \quad (16)$$

leads to the farfield radiation patterns  $D_w(\phi)$ ,  $D_{w,S}(\phi)$  and  $D_{w,S,H}(\phi)$  of finite length LSAs for a given temporal frequency  $\omega_0$ .  $D_{w,S}(\phi)$  is usually referred to as the *array factor* [10, p.45] or the *form factor* [3, II.2.a], whereas  $D_{w,S,H}(\phi)$  is termed *final array factor*, e.g. [18]. Those exclusively trigger the propagating part of the Green's function spatio-temporal spectrum [15, (52)]

$$G_0(x, k_y, \omega) = -\frac{j}{4} H_0^{(2)} \left( \sqrt{\left(\frac{\omega}{c}\right)^2 - k_y^2} \cdot x \right), \quad (17)$$

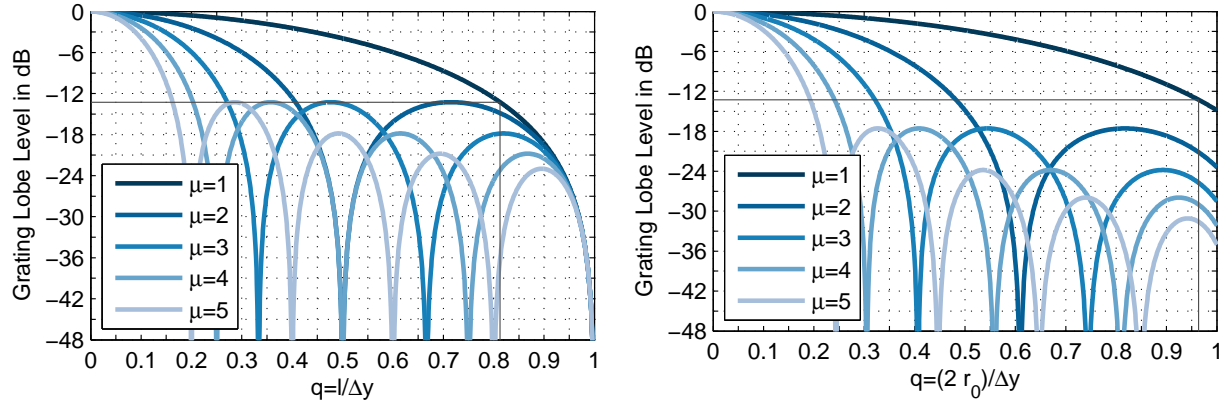
denoting the 0<sup>th</sup> order cylindrical Hankel function of 2<sup>nd</sup> kind [16, §10.2] as  $H_0^{(2)}(\cdot)$ . The propagating contributions of the sound field can be consequently obtained by inverse spatial Fourier transform

$$P(x, y, \omega) = \frac{1}{2\pi} \times \int_{-\frac{\omega_0}{c}}^{+\frac{\omega_0}{c}} \underbrace{D_{w,S,H}(k_y, \omega) G_0(x, k_y, \omega)}_{P(x, k_y, \omega)} e^{-j k_y y} dk_y, \quad (18)$$

which is known as the 'method of decomposition into wavelengths' [19, Ch. 13.5.4] and correctly synthesizes the sound fields of the Fresnel and Fraunhofer region. In (18) the LSA is exemplarily modeled with  $D_{w,S,H}(k_y, \omega)$  but any other LSA model can be employed with another driving function's spatio-temporal spectrum, cf. [2, (24,45)].

Grating lobes within the array factor that enter the visible region of the array are the most critical contributions to spatial aliasing. If not sufficiently suppressed, those contributions interfere with the intended main lobe beam. This results in a heavily corrupted Fresnel region, that was referred to as the *chaotic region* of an LSA [3, Fig. 16]. The sound field in this region is not amenable for equalization, since the sound pressure is highly dependent on the listener point and the frequency. The grating lobes furthermore are included in the farfield radiation pattern, as discussed above, which describes the Fraunhofer region of the LSA.

The first three WST criteria introduced different approaches for LSA applications (i) to completely avoid grating lobes within the visible region (WST#2) or (ii) to attenuate them, if entering into the visible region cannot be avoided (WST#1,#3).



(a) Line piston LSA, ARF =  $q$ , the ratio  $q = 0.812797$  with a resulting 1<sup>st</sup> grating lobe attenuation of 13.26 dB is indicated with lines.

(b) Circular piston LSA, ARF =  $\frac{\pi}{4} q^2$ , the ratio  $q = 0.9635792$  with a resulting 1<sup>st</sup> grating lobe attenuation of 13.26 dB is indicated with lines.

Fig. 3: Grating lobe level vs.  $q$  for (a) a line piston LSA and (b) a circular piston LSA. Relative grating lobe levels for  $k_y = \mu \frac{2\pi}{\Delta y}$ ,  $1 \leq \mu \leq 5$  are given. Only for a large number  $N$  of pistons this level corresponds to the real local maxima/minima of (19) and (25).

### 3. DISCUSSION OF WST #1:

The maximum tolerated grating lobe level of -13.5 dB relative to the intended main lobe can be understood as the essence of the 1<sup>st</sup> WST criterion (1). [3, 4, 5] concluded that this is only realizable with line pistons, i.e. waveguides. We present a discussion for both, the line and the circular piston for completeness.

#### 3.1. The ARF for a Line Piston LSA

The initial derivation of the ARF-theorem [3, (8)], [5, Sec. 3.2] was performed by defining a continuous, uniformly driven, finite length line source and a polarity-inverted *disruption grid* and thus, by inherently modeling a line piston LSA. We give another, yet consistent derivation using the product theorem (15) with (12) and (13)

$$D_{w,S,H}(k_y, \omega) = \frac{1}{N} \frac{\sin(k_y \Delta y N/2)}{\sin(k_y \Delta y/2)} \cdot \frac{\sin(k_y \frac{l}{2})}{k_y \frac{l}{2}}. \quad (19)$$

Finding the local minima and maxima, especially of grating lobes

$$\frac{dD_{w,S,H}(k_y, \omega)}{dk_y} = 0, \quad (20)$$

besides the main lobe, in order to minimize its largest occurring magnitude does not lead to a general closed form solution, which also holds for  $D_w(k_y)$  and  $D_{w,S}(k_y)$ . However, for large  $N$  the grating lobe maxima are approximately located at  $k_y = \mu \frac{2\pi}{\Delta y}$ ,  $\mu \in \mathbb{Z}, \neq 0$  in (19). The grating lobes decrease in level – except for the case  $l = 0$  – for increasing  $|k_y|$  due to the spatial lowpass characteristic of (13). Hence, the first grating lobes at  $|\mu| = 1$  determine the maximum occurring and tolerated level of grating lobes. With the initial definition [5, p.917]

$$\text{ARF} = q = \frac{l}{\Delta y} \quad 0 \leq q \leq 1 \quad (21)$$

(19) is evaluated at  $k_y = \Delta k_y = \frac{2\pi}{\Delta y}$  to

$$A(q) = D_{w,S,H}(k_y = \Delta k_y, \omega) = \frac{\sin(\pi q)}{\pi q}, \quad (22)$$

for which  $A(q) \in \mathbb{R}^+$  is valid for the given range of  $q$ . For  $q = 0$  a linear array built from spherical monopoles is modeled, due to the limit  $H_{\text{Rect}} = 1$ . All grating lobes will not be suppressed –  $D_{w,S,H}(k_y = \mu \Delta k_y, \omega) = 1$  – due to the missing spatial lowpass characteristic of a monopole. The limit  $q = 1$  perfectly suppresses all grating lobes –

$D_{w,S,H}(k_y = \mu \Delta k_y, \omega) = 0$  for  $\mu \neq 0$ , which furthermore leads to

$$D_w(k_y, \omega) = D_{w,S}(k_y, \omega) \cdot H_{\text{Rect}}(k_y, \omega)|_{l=\Delta y}, \quad (23)$$

i.e. the reconstruction towards the driving function's spectrum of the continuous, finite length LSA (10). Note that this perfect reconstruction holds only for  $\Delta y = l$  and the WST driving function (12), i.e. for wave radiation perpendicular to the LSA. Note also, that in this case the reconstruction is independent of the temporal frequency and of the chosen length  $\Delta y = l$ . The maximum tolerated grating lobe level thus can be controlled between 0 dB and  $-\infty$  dB by setting  $0 \leq q \leq 1$ . This is depicted in Fig. 3a.

In [3, 5] the maximum tolerated level of grating lobes was set to the largest occurring relative side lobe level of -13.26 dB<sup>2</sup> of a uniformly driven, continuous linear array, i.e. the maximum side lobe level of a continuous rectangular window. Therefore solving (22) for  $A(q) = 10^{-13.26/20}$  numerically, the ARF is given as

$$\text{ARF} = q \approx 0.812797. \quad (24)$$

This is in accordance with [5, p.917], where the approximation  $\text{ARF} \geq 0.82$  for large  $N$  is given. Note that (22) is independent of  $N$  in first instance. A discussed above, only for large  $N$  (19) exhibits also the local maximum at exactly  $k_y = \Delta k_y$ .

The ARF is a temporal frequency independent measure since the derivation was performed in the  $k_y$ -domain. The occurrence of (attenuated) grating lobes depends on the visible region  $-\frac{\omega_0}{c} < k_y < +\frac{\omega_0}{c}$  of the LSA. This indicates that if (2) can be fulfilled, the ARF criterion is of secondary importance and conversely, if (2) cannot be met, the grating lobe suppression is heavily dependent on the characteristics of the spatial reconstruction filter. An LSA with smaller  $\Delta y$  and smaller ARF may produce a better spatial-aliasing-free sound field for an intended frequency range, than an LSA with larger  $\Delta y$  and larger ARF. This is important realizing when aiming for electronic beam steering, that was initially not intended for the first LSA generation.

### 3.2. The ARF for a Circular Piston LSA

A treatment similar to Sec. 3.1 is given for the circular piston LSA. Applying the circular piston's

<sup>2</sup>To be precise, [3] uses -12dB and [5] uses -13.5 dB

postfilter characteristics (14) and the driving function (12) to the product theorem (15) yields

$$D_{w,S,H}(k_y, \omega) = \frac{1}{N} \frac{\sin(k_y \Delta y N/2)}{\sin(k_y \Delta y/2)} \cdot \frac{2 J_1(k_y r_0)}{k_y r_0}, \quad (25)$$

We define a ratio of lengths

$$q = \frac{d_0}{\Delta y} \quad 0 \leq q \leq 1, \quad (26)$$

by introducing the piston's diameter  $d_0 = 2 r_0$ . The ARF can be deduced to

$$\text{ARF} = \frac{\pi r_0^2}{\Delta y^2} = \frac{\pi \left(\frac{q}{2} \Delta y\right)^2}{\Delta y^2} = \frac{\pi}{4} q^2, \quad (27)$$

by modeling a quadratic enclosure of side length  $\Delta y$ . Note that the ARF here is truly a ratio of surface areas ( $\text{ARF} \neq q$ ), whereas for the line piston a ratio of line lengths is defined ( $\text{ARF} = q$ ). Therefore, care must be taken when comparing the definitions of the ARF and  $q$  and its implications.

Evaluating (25) at  $k_y = \Delta k_y = \frac{2\pi}{\Delta y}$  yields the relative level of the first grating lobe

$$A(q) = D_{w,S,H}(k_y = \Delta k_y, \omega) = \frac{2 J_1(\pi q)}{\pi q}. \quad (28)$$

The level of the first grating lobe ( $\mu = 1$ ) over  $q$  is depicted in Fig. 3b. For  $q = 1$  the maximum possible  $\text{ARF} = \pi/4$  is obtained for directly adjacent pistons  $\Delta y = d_0$ . This yields the maximum possible attenuation of grating lobes. For the first grating lobe (28) is evaluated to

$$A(q = 1) = \frac{2 J_1(\pi)}{\pi} \approx 0.181192, \quad (29)$$

which corresponds to -14.84 dB. This is in contrast to the line piston, for which perfect suppression ( $-\infty$  dB) of the first grating lobe (and all others) is achieved for  $q = 1$ . This due to the fact that the first zero of the Bessel function cannot be coincidentally located to  $k_y = \Delta k_y$  without overlapping pistons, which is physically not meaningful.

Regarding the initial intention of the 1<sup>st</sup> WST criterion, solving (28) for  $A(q) = 10^{-13.26/20}$  yields

$$q = 0.9635792 \quad \text{ARF} = \frac{\pi}{4} q^2 = 0.72923. \quad (30)$$

Hence, the circular piston postfilter is also able to attenuate the first grating lobe by 13.26 dB and therefore would be WST #1-compliant. This deduction is in contrast to that given in [3, 5]. In fact, the postfilter of the circular piston has a better spatial lowpass characteristic than the line piston since the Bessel function has a larger amplitude decay for increasing arguments than the  $\sin(x)/x$  function. This can also be graphically deduced in Fig. 3. Only for  $q \approx 1$  the grating lobe suppression for a line piston LSA is superior to a circular one.

While this discussion provides the whole picture of the ARF theorem from a theoretical viewpoint, LSAs nevertheless should be designed with waveguides for high audio frequencies due to the following reasons: (i) The circular piston model assumes a constant velocity over the membrane surface which is in practice much more demanding than designing an appropriate waveguide with an intended wavefront curvature; (ii) LSAs aim at a frequency independent horizontal coverage. This is much easier to control with the design of an appropriate waveguide than using circular pistons, i.e. electrodynamic loudspeakers.

#### 4. DISCUSSION OF WST #2:

Some recent LSA designs exhibit a very small source spacing  $\Delta y$  for high audio frequencies to shift spatial aliasing to very high audio frequencies and to relax the ARF requirements. Those LSA designs can be fixed straightly and aim at electronic beam forming and -steering, instead of controlling the LSA radiation characteristics with geometric curving. The most simple beam steering method is the delay-and-sum approach [10, Ch. 2.5], for which [17, p.175]

$$\Delta y < \frac{\lambda_{\min}}{2} \frac{N-1}{N} \quad (31)$$

ensures that no grating lobe beams enter the visible region for all possible steering angles  $|\phi_{\text{Steer}}| < 90^\circ$  of a rectangular windowed LSA built from spherical monopoles. For a very large source number  $N$  (31) merges into (2). Instead of using the spatial lowpass characteristics to avoid or attenuate spatial aliasing, this criterion relies on the limitation of the excitation signal's temporal frequency bandwidth. The condition (31) may be relaxed if only a limited steering angle  $|\phi_{\text{Steer}}| < |\phi_{\text{Steer,max}}|$  is allowed. For an infinite

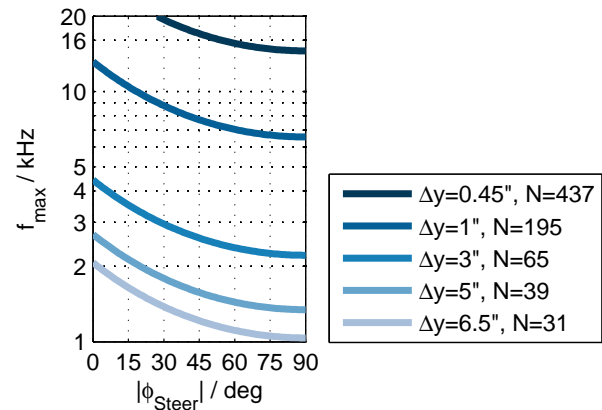


Fig. 4: Aliasing frequency over steering angle (33).

linear array [20, (10)], [15, (38)]

$$\Delta y < \frac{\lambda_{\min}}{1 + |\sin \phi_{\text{Steer,max}}|} \quad (32)$$

is known from SFS of a plane wave, as well as from antenna design [10, (2.129)]. For a finite length, rectangular windowed array with  $N$  spherical monopoles the condition reads

$$\Delta y < \frac{\lambda_{\min}}{1 + |\sin \phi_{\text{Steer,max}}|} \frac{N-1}{N}, \quad (33)$$

which is consistent with the result given in [21, (12)] for  $\phi_{\text{Steer}} = 0$ . Note that due to the non-linear mapping of  $k_y \leftrightarrow \phi$  the beamwidth broadens for increased  $\phi_{\text{Steer}}$  [10, Ch. 2.5], which is not further discussed here, since this paper is primarily interested in avoiding spatial aliasing.

For typical source spacings in LSA designs the maximum allowed frequency  $f_{\text{max}}$  for grating lobe free beam steering over the steering angle  $\phi_{\text{Steer}}$  is depicted in Fig. 4, assuming  $q = 1$ . The LSA length is always  $L \approx 5$  m. For the lowest audio frequencies typical larger electrodynamic loudspeakers are used and the range is approximately given as e.g.  $400 \text{ Hz} < f_{\text{max}} < 800 \text{ Hz}$  for  $90^\circ \geq \phi_{\text{Steer}} \geq 0^\circ$  ( $N = 13$ ,  $\Delta y = 15''$ ) and  $500 \text{ Hz} < f_{\text{max}} < 1000 \text{ Hz}$  for  $90^\circ \geq \phi_{\text{Steer}} \geq 0^\circ$  ( $N = 17$ ,  $\Delta y = 12''$ ). The low frequency band is thus uncritical for grating lobe free beam steering. However large waveguides of about the same dimension are not capable of pure electronic beam steering for high audio frequencies

due to the comparably low  $f_{\max}$  [2, 22]. Therefore such LSAs have to be curved geometrically in addition and delay-and-sum beamforming should there be avoided for the high frequencies. The mid-band of audio frequencies is very often driven by 5" or 6.5" speakers and an appropriate trade-off between the crossover lowpass cut-frequency and the allowed maximum steering angle has to be defined. The high-band of audio frequencies is still the most critical w.r.t. spatial aliasing and requires very small distances between drivers to avoid it. While this was not considered feasible when approaching LSA designs in the early 1990s for the first time, such techniques have been engineered nowadays. In the given example the 1"-piston would allow grating lobe free sound fields up to 10 kHz, when restricting  $|\phi_{\text{Steer,max}}| < 20^\circ$ , while the 0.45"-design would allow endfire beams up to 15 kHz.

## 5. DISCUSSION OF WST #3:

The 3<sup>rd</sup> WST criterion was derived for an LSA with directly adjacent horns (with no gaps) that exhibit a specified wavefront curvature (WFC). By discussing the 1<sup>st</sup> (1) and 3<sup>rd</sup> (3) WST criterion separately in [5, 13], one may erroneously assume that they are not interrelated. However, both criteria interact and determine the quality of grating lobe avoidance and suppression, which is discussed in this section.

### 5.1. Line Piston with Wavefront Curvature

Since a line piston with wavefront curvature exhibits a specific postfilter characteristics  $H_{\text{Post}}(k_y, \omega)$ , the discussion remains consistent within the signal processing in Fig. 2 by interpreting the resulting spatio-temporal spectrum  $D_{w,S,H}(k_y, \omega)$ . This discussion – based on the product theorem – was already given in [12, 13], however the farfield radiation pattern of a physically arc-shaped, uniformly driven source is utilized, i.e. the Huygens principle is applied. We propose to use Rayleigh-Sommerfeld diffraction of a baffled, infinitesimal narrow slit of finite length that is 'illuminated' by a point source. The wavefront curvature can be controlled by the point source position  $\mathbf{x}_{\text{PS}} = (-x_{\text{PS}}, 0, 0)^T$  behind the slit on  $y$ -axis, i.e. the distance  $x_{\text{PS}}$  in Fig. 1. With the line piston's length  $l$  and a desired wavefront curvature in terms of a wave length ratio  $S = \alpha \lambda$ , the geometric length

and angle relations

$$x_{\text{PS}} = \frac{l^2}{8S} - \frac{S}{2} = \frac{l^2}{8\alpha\lambda} - \frac{\alpha\lambda}{2}, \quad (34)$$

$$r = \frac{l^2}{8S} + \frac{S}{2} = \frac{l^2}{8\alpha\lambda} + \frac{\alpha\lambda}{2}, \quad (35)$$

$$\tan \phi = \frac{\frac{l}{2}}{\frac{l^2}{8S} - \frac{S}{2}} = \frac{\frac{l}{2}}{\frac{l^2}{8\alpha\lambda} - \frac{\alpha\lambda}{2}} \quad (36)$$

are derived according to Fig. 1. We require the distance  $x_{\text{PS}} > 0$ , which is valid if  $l^2/4 > (\alpha\lambda)^2$ .

SFS of a virtual point source using a linear, finite length, continuous secondary source distribution that models the slit is employed. The diffracted sound field is synthesized with [23, (16,31)]

$$P(\mathbf{x}, \omega) = \int_{-l/2}^{+l/2} D_{\text{WFC}}(y_0, \omega) G_N(\mathbf{x}, \mathbf{x}_0, \omega) dy_0, \quad (37)$$

using the slit  $\mathbf{x}_0 = (0, y_0, 0)^T$  on  $y$ -axis,  $\mathbf{x} = (x > 0, y, 0)^T$  and the 3D Neumann Green's function  $G_N(\mathbf{x}, \mathbf{x}_0, \omega) = 2G(\mathbf{x}, \mathbf{x}_0, \omega)$ . Using (34), the Spectral Division Method driving function [23, (24)]

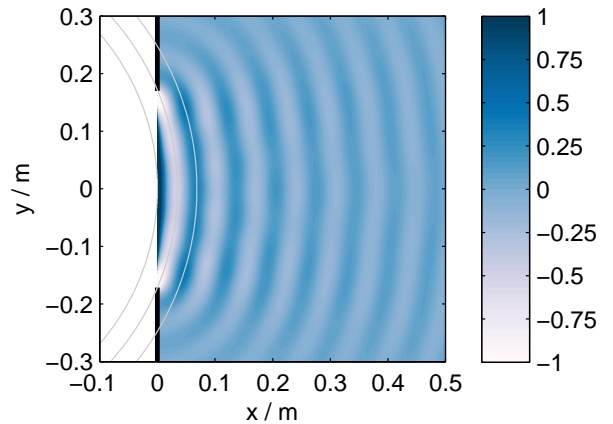


Fig. 5: Diffracted sound field  $\Re\{P(\mathbf{x}, \omega)\}$  of a point source synthesized by a baffled line piston with  $l = 0.343$  m for  $f = 5$  kHz using a wavefront curvature  $\alpha = 1/2$ ,  $x_{\text{PS}} = 0.4116$  m,  $\vartheta = 22.62^\circ$ ,  $c = 343$  m/s. Normalized to  $\Re\{P(\mathbf{x} = (\lambda/2, 0, 0)^T, \omega)\} = -1/2$ .

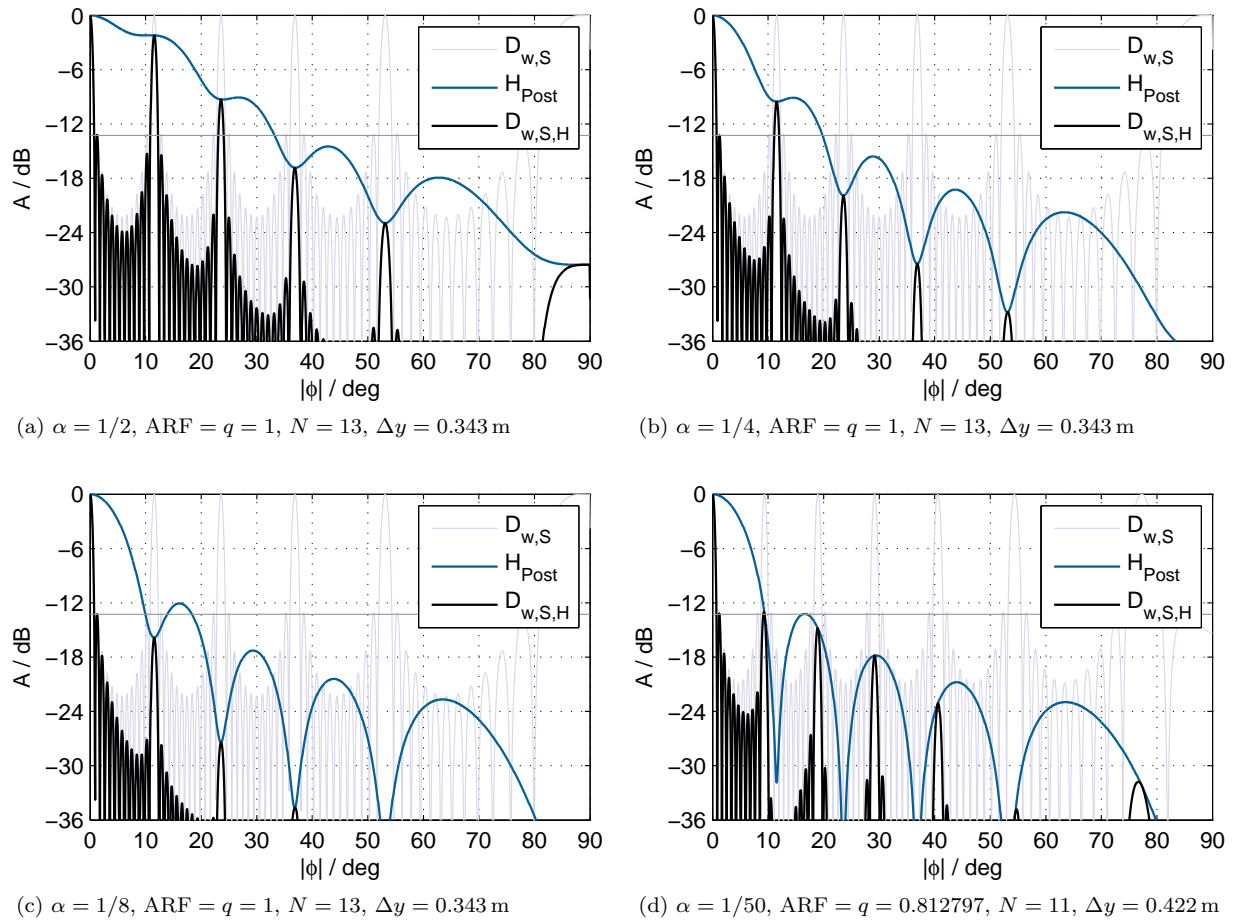


Fig. 6: Uniformly driven LSA with line pistons that exhibit a specified wavefront curvature. The excitation function  $D_{w,S}(\phi)$  (12), the postfilter  $H_{\text{Post}}(\phi)$  (39) and the resulting LSA farfield radiation pattern  $D_{w,S,H}(\phi) = D_{w,S}(\phi) \cdot H_{\text{Post}}(\phi)$  for  $f = 5$  kHz,  $l = 0.343$  m,  $c = 343$  m/s are visualized.

reads

$$D_{\text{WFC}}(y_0, \omega) = \frac{1}{4} \sqrt{\frac{x_{\text{ref}}}{x_{\text{ref}} + x_{\text{PS}}}} j \frac{\omega}{c} (-x_{\text{PS}}) \times \quad (38)$$

$$\frac{1}{\|\mathbf{x}_0 - \mathbf{x}_{\text{PS}}\|} \cdot H_1^{(2)}\left(\frac{\omega}{c} \|\mathbf{x}_0 - \mathbf{x}_{\text{PS}}\|\right),$$

denoting the Hankel function of second kind of order one as  $H_1^{(2)}(\cdot)$  [16, §10.2]. In contrast to Wave Field Synthesis driving functions [23, 24], (38) is also valid for point sources close to the slit, when the reference point  $x_{\text{ref}}$  – at which the sound field is to be synthesized correctly in amplitude and phase – is chosen

very large. This is in accordance for the quested farfield radiation pattern. Since the driving function is proportional to the normal source velocity, the spatial-temporal spectrum [19, Ch. 3.6]

$$H_{\text{WFC}}(k_y, \omega) = \int_{-l/2}^{+l/2} D_{\text{WFC}}(y_0, \omega) e^{+j k_y y_0} dy_0, \quad (39)$$

normalized to unity gain at  $k_y = 0$  for consistency, includes the farfield radiation pattern of the line piston with wavefront curvature. The integral is not

treatable for an analytic closed form solution and therefore numerical evaluation with a zero-padded FFT of the spatially discretized version of (38) is used. In Fig. 5 an example of the diffracted sound field for a wavefront curvature of  $\alpha = 1/2$  is given. The shown circles exhibit a radius increment of  $\lambda/2$ . One circle intersects the line piston in the origin and the subsequent circle with radius increment of  $\lambda/2$  intersects the line piston at its ends, which defines the sagitta  $S$ . In the following subsections the influence of the wavefront curvature w.r.t. grating lobe suppression is discussed for exemplarily chosen LSA setups and frequencies.

### 5.2. Single Waveguide LSA Element

For Fig. 6 different LSAs of about the same physical length  $L = (N - 1) \Delta y + l \approx 4.5$  m are modeled with line pistons of the same length  $l = 0.343$  m that exhibit different wavefront curvatures and ARF. The specific postfilters and the resulting LSA farfield radiation patterns over radiation angle  $\phi$  are depicted for  $f = 5$  kHz.

The line piston with  $\alpha = 1/2$  from Fig. 5 is used to model an ARF=1, N=13 LSA in Fig. 6a. The first grating lobes, with radiation angles  $\approx \pm 10^\circ$ , are attenuated by  $\approx 2$  dB (cf. [12, Fig. 20]), the second by 9 dB. For Fig. 6b the wavefront curvature is decreased to  $\alpha = 1/4$ , the maximum grating lobe level is about  $-10$  dB relative to the main lobe level (cf. [12, Fig. 19], [5, p.919]). According to the 3<sup>rd</sup> WST criterion (3),  $\alpha = 1/4$  is the maximum tolerated wavefront curvature, which however violates the 1<sup>st</sup> WST criterion (1) (min. 13.5 dB grating lobe suppression), even for ARF = 1.

A wavefront curvature of  $\alpha = 1/8$  is depicted in Fig. 6c (cf. [12, Fig. 18]). The maximum grating lobe level does not exceed approx.  $-16$  dB for ARF = 1 and approx.  $-11.5$  dB for ARF = 0.82. Hence, this wavefront curvature violates the 1<sup>st</sup> WST criterion for ARF = 0.82. In compliance with a tolerated maximum grating lobe level of  $-13.26$  dB a wavefront curvature of  $\alpha = 1/6$  is required, which however holds only for ARF  $\approx 1$ . If ARF = 0.82 is allowed, thus fulfilling the 1<sup>st</sup> WST criterion, the curvature  $\alpha > 1/50$  ensures the maximum allowed grating lobe level  $-13.26$  dB, as shown in Fig. 6d. For curvatures  $\alpha > 1/50$  the postfilter exhibits almost the same characteristics as the ideal line piston without wavefront curvature.

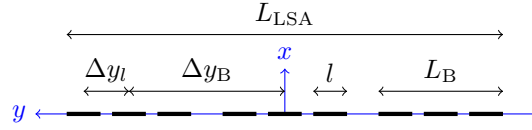


Fig. 7: Schematic sketch of an LSA built from  $N_B = 3$  boxes of physical height  $L_B$  spaced by  $\Delta y_B$ . Each box has  $N_l = 3$  line pistons of height  $l$  spaced by  $\Delta y_l$ . The total physical length of the LSA is  $L_{LSA}$ .  $N_B$  and  $N_l$  are assumed to be odd-numbered.

### 5.3. Multiple Waveguide LSA Box

The discussion above is valid for a single waveguide that spans about the entire height of a single LSA cabinet. In practical designs an LSA cabinet is often built from multiple and smaller waveguides each coupled to an individual compression driver, cf. Fig. 7. Ideally the waveguides should be driven individually, since this improves the capability for electronic beam forming, cf. Sec. 4. However, it is still common practice to drive high frequencies uniformly, i.e. all compression drivers per LSA cabinet get the same signal. For a uniformly driven, straight LSAs this can be modeled with the product theorem for nested arrays, also referred to as subarrays, cf. eg. [18]. The spatio-temporal spectrum is then given as

$$D_{w,S,H}(k_y, \omega) = \underbrace{\frac{1}{N_l} \frac{\sin(k_y \Delta y_l N_l / 2)}{\sin(k_y \Delta y_l / 2)}}_{D_{w,S,l}(k_y, \omega)} \cdot H_{\text{Post}}(k_y, \omega) \times \underbrace{\frac{1}{N_B} \frac{\sin(k_y \Delta y_B N_B / 2)}{\sin(k_y \Delta y_B / 2)}}_{D_{w,S,B}(k_y, \omega)}, \quad (40)$$

for which the first product models the farfield radiation pattern of a single LSA cabinet build from  $N_l$  pistons, each featuring the spatial postfilter characteristics  $H_{\text{Post}}(k_y, \omega)$  (39). The subsequent product using (12) then models the complete farfield radiation pattern of the LSA built from  $N_B$  cabinets. From Fig. 7 the geometrical relations between the individual ARFs and physical lengths are derived to

$$q_l = \frac{l}{\Delta y_l} \quad L_B = (N_l - 1) \Delta y_l + l, \quad (41)$$

$$q_B = \frac{L_B}{\Delta y_B} \quad L_{LSA} = (N_B - 1) \Delta y_B + L_B. \quad (42)$$

Due to the interaction of three spatial spectra, the discussion is slightly more complicated and for line pistons with wavefront curvature no closed form solution exists so far. We give some numerical examples of the farfield radiation pattern in Fig. 8 for an assumed highest operating frequency  $f = 16$  kHz for a 'multiple waveguides per cabinet'-LSA design. For Fig. 8a and Fig. 8b three rather large waveguides are used per LSA element and the wavefront curvature is varied. The chosen parameters closely match typical LSA designs, i.e.  $q_l = 1$  and  $\text{ARF} = q_B = 0.82$ . For Fig. 8c and Fig. 8d the waveguides are smaller, thus fitting more of them per LSA element and the  $\text{ARF} = q_B$  is varied, while  $q_l = 1$ .

For the chosen source spacing and frequency no LSA is grating lobe free, due to violating the 2<sup>nd</sup> WST criterion. The large wavefront curvature in Fig. 8a leads to grating lobes larger than  $-12$  dB for small radiation angles, which can be reduced when decreasing the curvature in Fig. 8b. When comparing Fig. 8b (large waveguides) and Fig. 8c (small waveguides) with otherwise same parameters, it is observed that the grating lobes at small angles  $\phi$  are more attenuated for the latter LSA, due to the larger decay of  $D_{w,S,1}(k_y, \omega)$ . It is worth realizing at this point, that grating lobes at small angles corrupt the intended sound field in a much larger spatial region than those radiated with large angles. This advantage, however comes with a comparably larger grating lobe level at  $|\phi| \approx 30^\circ$ . Due to the almost perfect coincidence of the aliased-sinc grating lobe maxima of  $D_{w,S,1}(k_y, \omega)$  (1st maximum) and  $D_{w,S,B}(k_y, \omega)$  (11th maximum) the postfilter only determines the attenuation level, which yields over 30 dB in Fig. 8b and about 16 dB in Fig. 8c. The coincidence of common maxima from  $D_{w,S,1}(k_y, \omega)$  and  $D_{w,S,B}(k_y, \omega)$  can be controlled by

$$q_B = \frac{q_l \cdot L_B}{\sigma \cdot l} \quad \sigma \geq N_l, \sigma \in \mathbb{N} \quad (43)$$

for which  $\sigma = N_l$  generally models  $q_B = 1$  if  $q_l = 1$ . This is an  $\text{ARF}=1$  LSA, for which the grating lobe suppression depends only on the spatial post-filter characteristics. The example in Fig. 8c closely matches  $\sigma = N_l + 2 = 9 + 2 \rightarrow q_B = 0.8\bar{1}$ . By increasing the ARF in Fig. 8d compared to Fig. 8c the grating lobes are generally more attenuated. Grating lobes at  $\approx 30^\circ$  differ significantly due to different

interaction of the involved functions.

In comparison to Sec. 5.2 larger wavefront curvature (in the example  $\alpha \leq 1/8$ ) is tolerated to fulfill the 1<sup>st</sup> WST criterion when using multiple smaller waveguides per LSA element. This is due to the additional spatial lowpass filter characteristic of  $D_{w,S,1}(k_y, \omega)$ , which compensates the insufficient lowpass characteristic of a waveguide with large wavefront curvature.

Despite the comparably large grating lobe level at about  $30^\circ$ , the LSAs in Fig. 8c, Fig. 8d could be preferred, due to the smaller discretization step (leaving more frequency bandwidth uncorrupted from aliasing, improved capability for electronic beam forming) and due to the larger decay of grating lobe levels for small radiation angles (larger spatial region without spatial aliasing).

## CONCLUSION

This paper presents an extended analysis to the first three Wavefront Sculpture Technology criteria for straight line source arrays, that deal with different approaches to avoid or reduce grating lobes. The correct ARF theorem for a circular piston array is furthermore given. For arrays with rather small source spacing the sampling theorem becomes important, when aiming at electronic beam forming and -steering. Meaningful radiation angles for steered arrays are given in terms of grating lobe avoidance. A line piston model for wavefront curvature is introduced and the subarray product theorem is applied to arrays which exhibit more than one waveguide per cabinet. In the latter case the allowed maximum wavefront curvature of a line piston is more relaxed.

## 6. REFERENCES

- [1] Schultz, F.; Rettberg, T.; Spors, S. (2014): "On spatial-aliasing-free sound field reproduction using infinite line source arrays." In: *Proc. of the 136th Audio Eng. Soc. Conv., Berlin*, #9078.
- [2] Schultz, F.; Rettberg, T.; Spors, S. (2014): "On spatial-aliasing-free sound field reproduction using finite length line source arrays." In: *Proc. of the 137th Audio Eng. Soc. Conv., Los Angeles*, #9098.

- [3] Heil, C.; Urban, M. (1992): "Sound fields radiated by multiple sound sources arrays." In: *Proc. of 92nd Audio Eng. Soc. Conv., Vienna*, #3269.
- [4] Urban, M.; Heil, C.; Baumann, P. (2001): "Wavefront Sculpture Technology." In: *Proc. of 111th Audio Eng. Soc. Conv., New York*, #5488.
- [5] Urban, M.; Heil, C.; Baumann, P. (2003): "Wavefront Sculpture Technology." In: *J. Audio Eng. Soc.*, **51**(10):912–932.
- [6] Start, E.W.; Valstar, V.G.; de Vries, D. (1995): "Application of spatial bandwidth reduction in Wave Field Synthesis." In: *Proc. of the 98th Audio Eng. Soc. Conv., Paris*, #3972.
- [7] Start, E.W. (1997): *Direct Sound Enhancement by Wave Field Synthesis*. Ph.D. thesis, Delft University of Technology.
- [8] Verheijen, E. (1997): *Sound Reproduction by Wave Field Synthesis*. Ph.D. thesis, Delft University of Technology.
- [9] Ahrens, J.; Spors, S. (2010): "On the anti-aliasing loudspeaker for sound field synthesis employing linear and circular distributions of secondary sources." In: *Proc. of the 129th Audio Eng. Soc. Conv., San Francisco*, #8246.
- [10] Van Trees, H.L. (2002): *Optimum Array Processing*. New York: Wiley.
- [11] Balanis, C.A. (2005): *Antenna Theory - Analysis and Design*. Hoboken: Wiley, 3. ed.
- [12] Ureda, M.S. (2001): "Line arrays: Theory and applications." In: *Proc. of 110th Audio Eng. Soc. Conv., Amsterdam*, #5304.
- [13] Ureda, M.S. (2004): "Analysis of loudspeaker line arrays." In: *J. Audio Eng. Soc.*, **52**(5):467–495.
- [14] Thompson, A. (2009): "Improved methods for controlling touring loudspeaker arrays." In: *Proc. of 127th Audio Eng. Soc. Conv., New York*, #7828.
- [15] Ahrens, J.; Spors, S. (2010): "Sound field reproduction using planar and linear arrays of loudspeakers." In: *IEEE Trans. Audio Speech Language Process.*, **18**(8):2038–2050.
- [16] Olver, F.W.J.; Lozier, D.W.; Boisvert, R.F.; Clark, C.W. (2010): *NIST Handbook of Mathematical Functions*. Cambridge University Press, 1. ed.
- [17] Stenzel, H. (1929): "Über die Richtcharakteristik von in einer Ebene angeordneten Strahlern." In: *Elektrische Nachrichtentechnik*, **6**(5):165–181.
- [18] Brockett, T.J.; Rahmat-Samii, Y. (2012): "Subarray design diagnostics for the suppression of undesirable grating lobes." In: *IEEE Trans. Antennas and Propagation*, **60**(3):1373–1380.
- [19] Möser, M. (2009): *Engineering Acoustics, An Introduction to Noise Control*. Dordrecht, Berlin, Heidelberg, New York: Springer, 2. ed.
- [20] Spors, S.; Rabenstein, R. (2006): "Spatial aliasing artifacts produced by linear and circular loudspeaker arrays used for wave field synthesis." In: *Proc. of the 120th Audio Eng. Soc. Conv., Paris*, #6711.
- [21] Stenzel, H. (1927): "Über die Richtwirkung von Schallstrahlern." In: *Elektrische Nachrichtentechnik*, **4**(6):239–253.
- [22] Meyer Sound Laboratories Inc. (2002): "DSP beam steering with modern line arrays." Tech. rep., [https://www.meyersound.com/pdf/support/papers/beam\\_steering.pdf](https://www.meyersound.com/pdf/support/papers/beam_steering.pdf), last seen on 2014-10-17.
- [23] Spors, S.; Ahrens, J. (2010): "Analysis and improvement of pre-equalization in 2.5-dimensional Wave Field Synthesis." In: *Proc. of the 128th Audio Eng. Soc. Conv., London*, #8121.
- [24] Spors, S.; Rabenstein, R.; Ahrens, J. (2008): "The theory of Wave Field Synthesis revisited." In: *Proc. of the 124th Audio Eng. Soc. Conv., Amsterdam*, #7358.

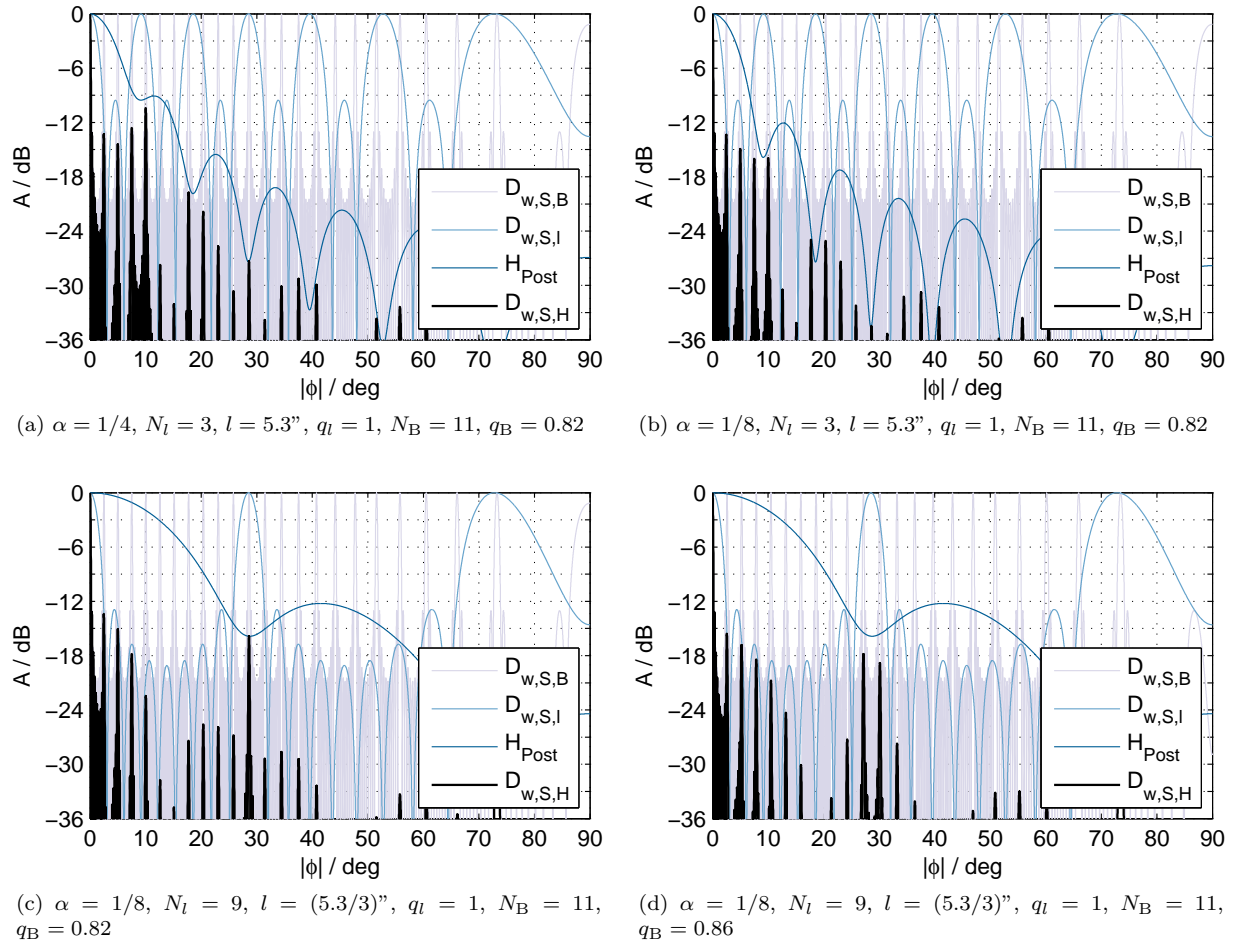


Fig. 8: Grating lobe levels over  $|\phi|$  for uniformly driven LSAs with line pistons of specified wavefront curvature  $\alpha$  using (40) with (38) and (39),  $f = 16$  kHz,  $c = 343$  m/s. Fig. a) and b) use  $3 \times 5.3''$  waveguides per LSA cabinet,  $\alpha$  is varied. Fig. c) and d) use  $9 \times 1.76''$  waveguides per LSA cabinet,  $q_B$  is varied.  $q_l = 1$  for all cases.